Mechanics of Time-Dependent Materials (2026) 30:40
https://doi.org/10.1007/s11043-026-09885-1

RESEARCH

Size dependent dynamics of a perforated Timoshenko nanobeam made of viscoelastic material with rotationally restrained ends

Hayrullah Gun Kadioglu[1] · **Mustafa Ozgur Yayli**[2]

Received: 13 March 2024 / Accepted: 12 May 2026
© The Author(s) 2026

Abstract
In this study, the free vibration behavior of perforated viscoelastic nonlocal Timoshenko beams has been investigated using a semi analytic method based on the Fourier series and the Stokes transformation. First, the geometric structure of the perforated beam was defined; then, by combining the Kelvin–Voigt viscoelastic model with the theory of nonlocal elasticity, the equations of motion describing the system were derived. During the solution phase, the boundary conditions of the beam were reduced to an eigenvalue problem using a semi analytic approach, with spring elements restricting rotation at both ends, and high-accuracy results have been obtained under various boundary conditions. The findings indicate that an increase in the nonlocal scale parameter has a softening effect on structural stiffness, thereby reducing vibration characteristics. Additionally, it is observed that an increase in the number of holes enhances discontinuity along the beam, leading to significant changes in system behavior. It is determined that the viscoelastic damping effect becomes more dominant, particularly under rigid boundary conditions, but weakens as the perforation density increases. The study also reveals that the void ratio, shear deformation, and boundary conditions are in strong interaction with one another. The proposed method offers an effective and reliable methodological approach for the dynamic analysis of perforated nanostructures, thanks to both its high convergence performance and its ability to model different boundary conditions within the same formulation.

Keywords Perforated beam · Timoshenko beam theory · Nonlocal elasticity theory · Free vibration · Viscoelastic · Damping

1 Introduction

Today, nanotechnology attracts the attention of researchers because it is used in many fields such as industry, mechanics, and electricity (Amir et al. 2019; Zhang et al. 2020). For this

✉ H.G. Kadioglu
hayrullahgunkadioglu@arel.edu.tr

1 Technical Sciences Vocational School, Department of Construction, İstanbul Arel University, İstanbul, Turkey

2 Faculty of Engineering, Department of Civil Engineering, Bursa Uludag University, Bursa, Turkey

Published online: 25 May 2026

reason, many researchers submit their work in this field (Uzun et al. 2020; Yayli 2018, 2016; r. Ebrahimian et al. 2018; Reddy 2011). However, working in this field is not as easy as it seems. Because the mechanical behavior of a material at the nanoscale is different from known classical mechanical behavior (Khaniki 2018). Hence, some theories such as nonlocal elasticity theory, nonlocal strain-gradient theory, and modified couple stress theory have been put forward to describe mechanical behavior at this nanoscale (Roudbari et al. 2022). One of the most well-known of these is Eringen's nonlocal elasticity theory. According to this theory, the stress at a point in the continuous medium is defined as a function of not only the deformation at that point but also the deformations at all points in the medium (Eringen and Edelen 1972; Eringen 1972). In this context many researchers working on nano structures have presented their studies by integrating nonlocal elasticity theory with different beam theories (Shanab et al. 2020; Mohamed et al. 2016; Reddy 2007; Trabelssi et al. 2019; Uymaz 2013; Nejad and Hadi 2016).

On the other hand, it is worth noting that for nanobeam modeling, another important size-dependent framework is strain-gradient elasticity theory, which accounts for both strain and its spatial gradients in the constitutive description. In particular, recent developments such as the strain-gradient-based Bernoulli–Euler beam model proposed by Zhang and Gao (2020) have displayed that such formulations can provide an alternative and, in some cases, more refined description of size effects.

Although there are many beam theories, the most notable beam theories are Euler Bernoulli and Timoshenko beam theories. According to Euler Bernoulli beam theory, sections that are plane and perpendicular to the neutral axis before bending remain perpendicular and plane to the neutral axis after bending. It is the most used and known beam theory because it has a straightforward and comprehensible mathematical expression (Eltaher et al. 2013). According to Timoshenko beam theory, a section that is plane and perpendicular to the neutral axis before bending remains plane to the neutral axis after bending but does not remain perpendicular (Kadıoğlu and Yaylı 2017). Since this theory also considers shear effects, it can be said to be an extended version of Euler Bernoulli beam theory.

Researchers can clearly explain behavior of such as bending, buckling, and torsion of nanoscale structures. However, this is not the case for dynamic behavior. In most studies, the damping effect is neglected. Because defining damping parameters is quite complex and difficult (Mohammadimehr et al. 2020). Nevertheless, it is also clear that damping has a significant effect on dynamic behavior (Karličić et al. 2015).

Some studies conducted in this context are summarized below:

Wang et al. (2007) presented an exact solution for free vibration analysis of nonlocal Timoshenko beams. Shen et al. (2012) carried out the vibration analysis of nano carbon tubes under clamped–free boundary conditions using the transfer function method. Abdullah et al. (2023) carried out the vibration analysis of nano carbon tubes under clamped–free boundary conditions using the transfer function method. Ke et al. (2009) studied the nonlinear free vibration of embedded double-walled carbon nanotubes, and the differential quadrature method was employed to solve the governing equations. Ghadiri et al. (2016) carried out the vibration analysis of rotational nanobeams under thermal effects using force series. Azimi et al. (2018) performed free vibration analysis of rotating functionally graded nanosized Timoshenko beams with nonlinear thermal distribution using the differential quadrature method. Czekanski and Zozulya (2021) studied the free and forced vibrations of nanoscale beams using higher order beam theories. They have proposed Navier's analytic closed-form solution. Yayli (2014) examined the axial vibration of carbon nanotubes under elastic boundary conditions using Fourier series. Murmu and Adhikari (2010) obtained a closed solution using an analytical method for the solution of axial vibration of non-local double beams.

Artan and Tepe (2025) developed a new and computationally efficient semi-analytical solution method based on nonlocal elasticity for the behavior of curved nanobeams. Tepe (2025) analyzed the mechanical behavior of curved double-walled carbon nanotubes within the framework of nonlocal elasticity by combining the initial value method with the approximate transfer matrix approach. Civalek et al. (2025) analyzed the size effects of nano-scale rings embedded in an elastic medium for the first time within the framework of nonlocal elasticity, investigated their free vibration behavior, and derived the frequency equations. Dalgıç et al. (2025) solved the static behavior of helical SWCNT beams in closed form for the first time within the framework of nonlocal Euler–Bernoulli theory, analytically deriving the translational and rotational components in the Frenet coordinate system. Hosseini et al. (2022) proposed a new solution method to investigate the dynamic responses of functionally graded nonlocal beams under moving loads. Challamel et al. (2025) studied the static bending behavior of nanobeams involving high-order shear deformation within the framework of nonlocal elasticity, reducing the equations of motion to a single sixth-order differential equation and obtaining exact closed-form solutions for various boundary conditions. Sheykhi et al. (2023) investigated the free vibration behavior of a nonlocal Euler–Bernoulli nanobeam interacting with a fluid, modeled the fluid–solid interaction forces using a Navier–Stokes-based approach, and analyzed how the vibration characteristics change in different fluid environments by solving the problem using the Galerkin method.

Uzun and Yaylı (2020) carried out the free vibration analysis of functionally graded nano beams based on two parameters resting on a Winkler elastic foundation, using the finite element method, which is used as a popular solution method today. Additionally, Uzun et al. (2023) studied a free vibration analysis of nonlocal Euler Bernoulli beams resting on one parameter Winkler elastic foundation by creating a stiffness and mass matrix. Abdelrahman et al. (2023) examined the dynamic behavior of carbon nanotubes sitting on elastic foundations under the influence of moving loads. Hamilton's principle has been used to create the equations of motion. In solving the problem, an analytical solution has been put forward using Navier procedures. Lee and Chang (2010) investigated the influence of surface effects on the vibrations of nonlocal Timoshenko beams.

Lei et al. (2013a) performed free vibration analysis of nonlocal viscoelastic Euler Bernoulli beams using the transfer function method. Additionally, using this method, a solution has been presented according to Timoshenko beam theory by Lei et al. (2013b). Ansari et al. (2015) investigated free vibration of fractional viscoelastic nonlocal Timoshenko beams with a numerical method. Attia and Abdel Rahman (2018) studied free vibration of functionally graded viscoelastic nanobeams under surface effect. Nonlinear vibration analysis of fractional nonlocal viscoelastic nanotube based on Kelvin-Voigt has been performed by proposing an iteration method using Laplace transform, Bessel functions and binomial series by Martin (2022). Hosseini-Hashemi et al. (2020) investigated the effects of surface effects on the dynamic behavior of viscoelastic nanobeams. Eltaher et al. (2019) studied the bending and vibration behaviors of piezoelectric nonlocal beams using the finite element method. Kadioglu and Yayli (2025) investigated the axial vibration behavior of functionally graded viscoelastic nanorods using the theory of nonlocal elasticity with Fourier series and Stokes transformation method. In addition, Kadioglu (2026) significantly addressed the existing limitations of the approach based on the Fourier series and the Stokes transform in his study, thereby expanding the method's applicability. Tariq et al. (2025) addressed the free vibration behavior of functionally graded viscoelastic Euler–Bernoulli beams within the framework of nonlocal theory; they developed semi-analytical solution approaches and conducted a comprehensive analysis using machine learning methods. Son et al. (2025) investigated the damped vibration behavior of functionally graded sandwich nanoplates resting on

a viscoelastic foundation using nonlocal elasticity and high-order shear deformation theory, and has evaluated the effect of different viscoelastic foundation models through parameter studies.

Using lighter and more rigid materials has always been the main goal of engineering. Perforated beams serve this purpose(Assie et al. 2021). Thus, it has been a significant research topic for researchers. Eltaher et al. (2023) carried out the free vibration analysis of nonlocal viscoelastic perforated beams using a numerical method.

This study has contributed significantly to literature by presenting a comprehensive model that examines the free vibration behavior of perforated viscoelastic nonlocal Timoshenko nanobeams. In this study, nonlocal elasticity theory, viscoelastic material behavior, shear deformation, and perforation effects are addressed together within the same mathematical formulation, thereby modeling the dynamic behavior of nanostructured materials more realistically. Furthermore, through a semi-analytical solution approach based on the Fourier series and the Stokes transform, the high-order coupled differential equation system is effectively reduced to a single eigenvalue problem, thereby achieving both high convergence performance and reliable results under various boundary conditions. In particular, the ability to model different support conditions within the same solution framework using elastic rotation springs enhances the flexibility and applicability of the proposed method. In this regard, the study presents an effective, reliable, and computationally efficient alternative methodological approach that can be utilized in the vibration analysis of perforated nanostructures.

2 Definition of the problem

In this section, the equations of motion for viscoelastic perforated Timoshenko nanobeams are derived. To this end, it is first necessary to define the beam's geometric structure and the basic model assumptions. In this context, the nanobeam model used as the basis for the analysis is displayed schematically in Fig. 1, and this geometric structure will be taken into account in deriving the equations of motion.

The parameters h, b, l_s and t_s in this beam model represent the beam height, the beam width, the period length, and the spatial period, respectively. Utilizing these parameters, the filling ratio of the perforated beam (a) is defined as follows (Eltaher et al. 2023).

$$a = \frac{t_s}{l_s} 0 \leq a \leq 1 \tag{1}$$

a takes values between zero and one. When a equals one, it indicates a partially filled beam. Below, the proportional expressions of the bending stiffness $(EI)_p$, shear stiffness $(GA)_p$,

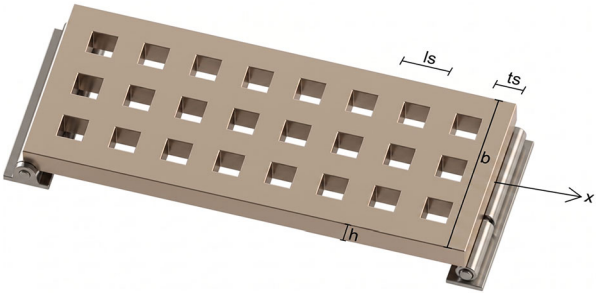


Fig. 1 Perforated nanobeam model

mass, and mass moment of inertia of the perforated beams compared to the solid beam are presented, respectively (Eltaher et al. 2023).

$$s_{EI} = \frac{(EI)_p}{EI} = \frac{a(N+1)(N^2+2N+a^2)}{\left(1-a^2+a^3\right)N^3+3aN^2+\left(3+2a-3a^2+a^3\right)a^2N+a^3} \tag{2}$$

$$s_{GA} = \frac{(GA)_p}{GA} = \frac{a^3(N+1)}{2N} \tag{3}$$

$$s_{\rho A} = \frac{(\rho A)_p}{\rho A} = \frac{(1-N\,(a-2))\,a}{N+a} \tag{4}$$

$$s_{\rho I} = \frac{(\rho I)_p}{\rho I} = \frac{a((2-a)\,N^3+3N^2-2\,(a-3)\left(a^2-a+1\right)N+a^2+1)}{(N+a)^3} \tag{5}$$

where E, G, ρ, A, I refer to the elasticity module, the shear module, the density, the cross-sectional area, and the moment of inertia respectively. N is the number of holes throughout the cross section. This concludes the description of the nanobeam's geometric properties.

Classical elasticity theories are often insufficient for investigating the dynamic behavior of micro and nano scale structural elements. The primary reason for this is that, as dimensions are reduced to micro and nano levels, behaviors known as the scale effect which cannot be explained by classical continuous media theories emerge in structural elements. For this reason, the nonlocal elasticity theory, which can account for small-scale effects, stands out as an effective approach widely used in the vibration analysis of nano-scale structures. According to the nonlocal theory, strain at a given point depends not only on the mechanical state at that point but is also influenced by interactions with neighboring points. In this context, this study also adopts the nonlocal elasticity theory to enable a more accurate modeling of behavior at the nano scale.

In light of this knowledge the moment (M) and shear force (V) function of based on Kelvin–Voigt model viscoelastic nonlocal Timoshenko beams are as follows (Eltaher et al. 2023).

$$M = (s_{EI})EI\left(1+t_d\frac{\partial}{\partial t}\right)\frac{\partial\theta}{\partial x}+\gamma\left((s_{\rho A})\rho A\frac{\partial^2\varphi}{\partial t^2}+(s_{\rho I})\rho I\frac{\partial^3\theta}{\partial x\partial t^2}\right) \tag{6}$$

$$V = (s_{GA})K_SGA\left(1+t_d\frac{\partial}{\partial t}\right)\left(\frac{\partial\varphi}{\partial x}+\theta\right)+\gamma\left((s_{\rho A})\rho A\frac{\partial^3\varphi}{\partial x\partial t^2}\right) \tag{7}$$

where φ and θ are vertical displacement and rotation functions respectively. K_S, t_d and γ are the shear correction coefficient, viscoelastic damping coefficient, scaling effect parameter respectively. Additionally, x represents the position, and t represents the time. Using shear force and moment, the equations of motion of viscoelastic nonlocal perforated Timoshenko beams are found as follows (Eltaher et al. 2023).

$$-(s_{GA})K_SGA\left(1+t_d\frac{\partial}{\partial t}\right)\left(\frac{\partial^2\varphi}{\partial x^2}+\frac{\partial\theta}{dx}\right)+(s_{\rho A})\rho A\left(1-\gamma\frac{\partial^2}{\partial x^2}\right)\frac{\partial^2\varphi}{\partial t^2}=0 \tag{8}$$

$$-(s_{EI})EI\left(1+t_d\frac{\partial}{\partial t}\right)\frac{\partial^2\theta}{\partial x^2}+(s_{GA})K_SGA\left(1+t_d\frac{\partial}{\partial t}\right)\left(\frac{\partial\varphi}{\partial x}+\theta\right)$$
$$+(s_{\rho I})\rho I\left(1-\gamma\frac{\partial^2}{\partial x^2}\right)\frac{\partial^2\theta}{\partial t^2}=0 \tag{9}$$

By utilizing the above motion equations, it is possible to identify the factors that determine the free vibration behavior of viscoelastic perforated nanobeams.

3 Solution method

In this section, the solution methodology for the problem is presented in detail. To this end, the equations of motion, which are initially expressed in the form of partial differential equations, must first be reduced to ordinary differential equations using appropriate transformations. In this context vertical displacement and rotation functions are as follows.

$$\varphi(x,t) = \varphi(x)\, e^{i\omega t} \tag{10}$$

$$\theta(x,t) = \theta(x)\, e^{i\omega t} \tag{11}$$

When these vertical displacement and rotation functions are put into the governing equations, the governing equations take the following form depending on the position.

$$\begin{aligned} &-(s_{\rho A})\rho A\omega^2\varphi + ((s_{\rho A})\rho A\omega^2\gamma - (s_{\mathrm{GA}})K_S GA(1+i\omega t_d))\frac{d^2\varphi}{dx^2} \\ &\quad + (-(s_{\mathrm{GA}})K_S GA(1+i\omega t_d))\frac{d\theta}{dx} = 0 \end{aligned} \tag{12}$$

$$\begin{aligned} &\left(-\left(s_{\rho \mathrm{I}}\right)\rho I\omega^2 + (s_{\mathrm{GA}})\, K_S GA\,(1+i\omega t_d)\right)\frac{d\theta}{dx} \\ &\quad + \left((s_{\mathrm{EI}})\, EI\,(1+i\omega t_d) + \left(s_{\rho \mathrm{I}}\right)\rho I\omega^2\gamma\right)\frac{d^3\theta}{dx^3} \\ &\quad + ((s_{\mathrm{GA}})K_S GA\,(1+i\omega t_d))\,\frac{d^2\varphi}{dx^2} = 0 \end{aligned} \tag{13}$$

A simplification has been made in solving the problem by expressing the governing equations as follows.

$$H_a\varphi + H_b\frac{d^2\varphi}{dx^2} + H_c\frac{d\theta}{dx} = 0 \tag{14}$$

$$H_d\frac{d\theta}{dx} + H_e\frac{d^3\theta}{dx^3} + H_f\frac{d^2\varphi}{dx^2} = 0 \tag{15}$$

where H_a, H_b, H_c, H_d, H_e and H_f are presented below.

$$H_a = -(s_{\rho A})\rho A\omega^2 \tag{16a}$$

$$H_b = (s_{\rho A})\rho A\omega^2\gamma - (s_{GA})K_S GA\,(1+i\omega t_d) \tag{16b}$$

$$H_c = -(s_{GA})K_S GA\,(1+i\omega t_d) \tag{16c}$$

$$H_d = -(s_{\rho I})\rho I\omega^2 + (s_{GA})K_S GA\,(1+i\omega t_d) \tag{16d}$$

$$H_e = -(s_{EI})EI\,(1+i\omega t_d) + (s_{\rho I})\rho I\omega^2\gamma \tag{16e}$$

$$H_f = (s_{GA})K_S GA(1+i\omega t_d) \tag{16f}$$

Various numerical, semi analytic and analytic methods can be employed to solve the differential equations derived above. Each method has its own unique advantages and limitations.

In this study, however, the Fourier series and Stokes transform method a semi-analytic approach has been preferred due to its ability to reduce the problem to a single eigenvalue problem, its high convergence performance, and its ability to provide reliable results.

Similar simplification has been done in the moment function.

$$M = \left((s_{EI})EI\,(1 + i\omega t_d) - (s_{\rho I})\rho I\omega^2\gamma\right)\frac{d\theta}{dx} - (s_{\rho A})\rho A\omega^2\gamma\varphi \tag{17}$$

$$M = H_g\frac{d\theta}{dx} + H_h\varphi \tag{18}$$

where H_g and H_h are indicated below.

$$H_g = EI + t_d i\omega EI - \gamma\rho I\omega^2 \tag{19a}$$

$$H_h = -(s_{\rho A})\rho A\omega^2\gamma \tag{19b}$$

For the solution process to begin, the rotation and vertical translation functions must be represented by Fourier series. In this context, Fourier sine series has been selected for the vertical displacement function and Fourier cosine series has been selected for the rotation function. Defining rotation and vertical displacement functions in this way might, at first glance, give the impression that the solution approach is valid only for simply supported beams. However, thanks to the higher-order independent derivatives obtained using Stokes' transformations, it is possible to obtain solutions for beams with different boundary conditions as well. Higher order derivatives of these functions using Stokes transformations are presented below (Kadıoğlu and Yaylı 2017).

$$\alpha_m = \frac{m\pi}{L} \tag{20}$$

$$\varphi = A_m \mathrm{Sin}[\alpha_m x] \tag{21}$$

$$\frac{d\varphi}{dx} = \frac{\varphi_L - \varphi_0}{L} + \sum_{m=1}^{\infty}\left(\frac{2}{L}\left(\varphi_L\,(-1)^m - \varphi_0\right) + \alpha_m A_m\right)\mathrm{Cos}\left[\alpha_m x\right],\ \varphi\,(0) = \varphi_0,\quad \varphi\,(L) = \varphi_L \tag{22}$$

$$\frac{d^2\varphi}{dx^2} = -\sum_{m=1}^{\infty}\alpha_m\left(\frac{2}{L}(\varphi_L(-1)^m - \varphi_0) + \alpha_m A_m\right)\mathrm{Sin}[\alpha_m x] \tag{23}$$

$$\theta = \sum_{m=1}^{\infty} B_m \mathrm{Cos}[\alpha_m x] \tag{24}$$

$$\frac{d\theta}{dx} = -\sum_{m=1}^{\infty}\alpha_m B_m \mathrm{Sin}[\alpha_m x] \tag{25}$$

$$\frac{d^2\theta}{\partial x^2} = \frac{\theta'_L - \theta'_0}{L} + \sum_{m=1}^{\infty}\left(\frac{2}{L}\left(\theta_L^{\prime(-1)^m} - \theta'_0\right) - \alpha_m^2 B_m\right)\mathrm{Cos}\left[\alpha_m x\right],\ \theta'\,(0) = \theta'_0,\quad \theta'\,(L) = \theta'_L \tag{26}$$

$$\frac{d^3\theta}{\partial x^3} = \sum_{m=1}^{\infty}\left(\frac{2}{L}\alpha_m(\theta'_0 - \theta'_L(-1)^m) + \alpha_m^3 B_m\right)\mathrm{Sin}[\alpha_m x] \tag{27}$$

where A_m and B_m are the Fourier coefficients. L is the length of beam. The above functions are placed in the governing Eqs. (14)–(15) and the Fourier coefficients are found as follows.

$$A_m = (2\alpha_m(-H_b H_d \varphi_0 + H_c H_f \varphi_0 + H_b H_e \alpha_m^2 \varphi_0 + (-1)^m H_b H_d \varphi_L + (-1)^{1+m} H_c H_f \varphi_L + (-1)^{1+m} H_b H_e \alpha_m^2 \varphi_L + H_c H_e \theta_0' + (-1)^{1+m} H_c H_e \theta_L')) / L(H_a H_d - H_b H_d \alpha_m^2 - H_a H_e \alpha_m^2 + H_c H_f \alpha_m^2 + H_b H_e \alpha_m^4) \tag{28}$$

$$B_m = -(2\left(-H_a H_f \varphi_0 + (-1)^m H_a H_f \varphi_L - H_a H_e \theta_0' + H_b H_e \alpha_m^2 \theta_0' + (-1)^m H_a H_e \theta_L' + (-1)^{1+m} H_b H_e \alpha_m^2 \theta_L'\right)) / L(H_a H_d - H_b H_d \alpha_m^2 - H_a H_e \alpha_m^2 + H_c H_f \alpha_m^2 + H_b H_e \alpha_m^4) \tag{29}$$

Using Eq. (15), the rotation function can be expressed as follows.

$$\theta = -\frac{H_e}{H_d}\frac{d^2\theta}{dx^2} - \frac{H_f}{H_d}\frac{d\varphi}{dx} \tag{30}$$

Consider the boundary conditions illustrated in Fig. 2, the moment function can be expressed as follows.

$$M = R\theta = H_g \frac{d\theta}{dx} + H_h \varphi \tag{31}$$

where R is rotation stiffness. A matrix of coefficients can be created by arranging the above equations as follows and specifying the boundary conditions.

$$\text{for } x = 0,\ R_1\left(\frac{H_e}{H_d}\frac{d^2\theta}{dx^2} + \frac{H_f}{H_d}\frac{d\varphi}{dx}\right) + H_g\frac{d\theta}{dx} + H_h\varphi = 0 \tag{32}$$

$$\text{for } x = L,\ R_2\left(\frac{H_e}{H_d}\frac{d^2\theta}{dx^2} + \frac{H_f}{H_d}\frac{d\varphi}{dx}\right) - H_g\frac{d\theta}{dx} - H_h\varphi = 0 \tag{33}$$

Here, R_1 and R_2 represent the stiffness of the elastic springs that restrict rotation at $x = 0$ and $x = L$, respectively. By incorporating the other boundary conditions indicated in Fig. 2 into these two equations, they can be represented in the form of a 2×2 matrix as follows.

$$x = 0 \rightarrow \alpha_m = \frac{m\pi}{L};\ \varphi_0 = 0;\ \varphi_L = 0 \tag{34}$$

$$x = L \rightarrow \alpha_m = \frac{m\pi}{L};\ \varphi_0 = 0;\ \varphi_L = 0 \tag{35}$$

$$\begin{bmatrix} \Phi_{11} & \Phi_{12} \\ \Phi_{21} & \Phi_{22} \end{bmatrix} \begin{bmatrix} \theta_0' \\ \theta_L' \end{bmatrix} = 0 \tag{36}$$

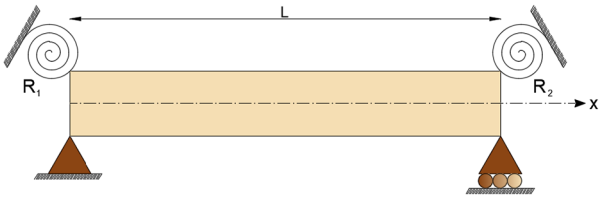


Fig. 2 Perforated nonlocal viscoelastic Timoshenko beam's boundary condition

$$\Phi_{11} = \frac{-R_1 H_e}{L H_d} + H_g + \sum_{m=1}^{\infty} \frac{2L(-L^2 H_a + m^2\pi^2 H_b) H_e R_1}{(L^2 H_a - m^2\pi^2 H_b)(L^2 H_d - m^2\pi^2 H_e) + L^2 m^2\pi^2 H_c H_f} \tag{36a}$$

$$\Phi_{12} = \frac{R_1 H_e}{L H_d} + \sum_{m=1}^{\infty} \frac{2(-1)^m L(L^2 H_a - m^2\pi^2 H_b) H_e R_1}{(L^2 H_a - m^2\pi^2 H_b)(L^2 H_d - m^2\pi^2 H_e) + L^2 m^2\pi^2 H_c H_f} \tag{36b}$$

$$\Phi_{21} = \frac{-R_2 H_e}{L H_d} + H_g + \sum_{m=1}^{\infty} \frac{2L(-L^2 H_a + m^2\pi^2 H_b) H_e R_2}{(L^2 H_a - m^2\pi^2 H_b)(L^2 H_d - m^2\pi^2 H_e) + L^2 m^2\pi^2 H_c H_f} \tag{36c}$$

$$\Phi_{22} = \frac{R_2 H_e}{L H_d} + \sum_{m=1}^{\infty} \frac{2(-1)^m L(L^2 H_a - m^2\pi^2 H_b) H_e R_2}{(L^2 H_a - m^2\pi^2 H_b)(L^2 H_d - m^2\pi^2 H_e) + L^2 m^2\pi^2 H_c H_f} \tag{36d}$$

The natural frequencies can be obtained by setting the determinant of the 2×2 system in the matrix equation above equal to zero. However, in these calculations, the series that make up the matrix elements theoretically contain an infinite number of terms. In practice, however, the series must be truncated at a certain number of terms to enable a numerical solution. The number of terms to be used is determined as the most appropriate value based on a convergence analysis conducted to ensure the accuracy of the results.

4 Result and discussion

In this section, the parameters affecting the free vibration of viscoelastic perforated Timoshenko nanobeams are analyzed and discussed in detail. First of all, to compare the results with studies in literature, the dimensionless frequency parameter presented below has been used in this study.

$$\lambda = \omega L^2 \sqrt{\frac{\rho A}{E I}} \tag{37}$$

Before presenting the results regarding the dimensionless frequency parameters defined above, it is necessary to explain how the boundary conditions have been incorporated into the model. In this context, to represent the simply supported (S-S) boundary condition, a very small value of 10^{-9} has been assigned to both spring constants, which represent rotational stiffness. For the clamped-clamped (C-C) boundary condition, both spring constants have been selected as 10^9 to significantly restrict rotational motion. In the analysis conducted, it has been observed that further increasing or decreasing these values does not cause a significant change in the frequencies therefore, these values have been deemed sufficient. In the clamped–simple support (C-S) boundary condition, one spring constant has been defined as 10^{-9} and the other as 10^9.

On the other hand, the importance of convergence analysis for the solution method to yield reliable and optimal results has been discussed in the previous section. Since comprehensive convergence analyses have already been conducted in similar studies based on the Fourier series and Stokes transform methods, a detailed convergence analysis is not presented in this study. Instead, as suggested in the work of Kadioglu (2026), the calculations have been performed using 1000 terms to ensure sufficient accuracy.

Table 1 Comparison of the dimensionless frequency parameter of nonlocal Timoshenko beams (L = 10, L/h = 10, E = 30 MPa $\rho = 1$, $\nu = 0.3$, $\tau = 0$)

Studies	γ	Simply supported			Clamped supported		
		Mode 1	Mode 2	Mode 3	Mode 1	Mode 2	Mode 3
Present	0	9.7076	37.0962	78.1548	20.9738	53.7500	97.1477
Trabelssi et al. (2019)		9.7075	37.0962	78.1547	20.9723	53.7468	97.1430
Reddy (2007)		9.7454	–	–	–	–	–
Present	0.5	9.4766	33.9009	65.0357	20.3677	48.6032	80.0521
Trabelssi et al. (2019)		9.4765	33.9009	65.0357	20.3663	48.6004	80.0486
Reddy (2007)		9.5135	–	–	–	–	–
Present	1	9.2613	31.4106	56.8754	19.8094	44.6723	69.6309
Trabelssi et al. (2019)		9.2612	31.4105	56.8753	19.8080	44.6699	69.6280
Reddy (2007)		9.2973	–	–	–	–	–
Present	1.5	9.0601	29.3990	51.1746	19.2928	41.5487	62.4506
Trabelssi et al. (2019)		9.0600	29.3991	51.1746	19.2916	41.5466	62.4482
Reddy (2007)		9.0953	–	–	–	–	–
Present	2	8.8714	27.7304	46.9034	18.8134	38.9919	57.1244
Trabelssi et al. (2019)		8.8713	27.7303	46.9034	18.8121	38.9900	57.1223
Reddy (2007)		8.9059	–	–	–	–	–

In Table 1, the results found in the literature for nonlocal Timoshenko beams and the results found in this study are presented. The results presented in the table demonstrate satisfactory agreement in terms of the accuracy and adequacy of the obtained solution.

Furthermore, a significant decrease in frequency values is observed as the scale parameter increases. It is believed that this phenomenon stems from the softening effect that the nonlocal scale parameter exerts on structural stiffness. However, it is observed that the decrease in frequency is more pronounced under stiffer boundary conditions. Since the effect of the scale parameter on structural behavior is felt more strongly in systems with high stiffness, the increase in the softening effect of the nonlocal parameter can be considered an expected and physically meaningful result.

In Table 2, the results for nonlocal viscoelastic perforated Timoshenko beams are compared. In this context, viscoelastic damping parameter (τ) is expressed as below.

$$\tau = \frac{t_d}{L^2\sqrt{\frac{\rho A}{EI}}} \tag{38}$$

The dimensionless frequency parameters obtained consist of imaginary and real parts for $\tau > 0$. In the results presented in this study, only real parts are presented. The results appear to be quite consistent, also some inferences can be made from Table 2. As the viscoelastic damping parameter and the number of holes increase, the dimensionless frequency parameter decreases. It is considered that the increase in the viscoelastic damping parameter leads to energy dissipation within the material, resulting in a decrease in the frequency values. On the other hand, it can be argued that the decrease in frequencies is an expected behavior, as the increase in the number of holes increases structural discontinuities along the beam,

Table 2 Dimensionless frequency parameters of viscoelastic nonlocal perforated Timoshenko beams under different boundary conditions and number of holes. ($h = 1$ nm, $h = b$, $L = 10$ nm, $E = 30$ MPa, $\nu = 0.3$, $\rho = 1$, $\alpha = 0.2$, $\gamma = 5$)

B.C.	N	$\tau = 0.02$			$\tau = 0.05$		
		λ1	λ2	λ3	λ1	λ2	λ3
S-S	1	5.49140	8.84336	10.0770	5.44749	8.65696	9.79893
	4	4.52503	7.52880	8.65449	4.50055	7.41462	8.47997
	8	4.28777	7.23125	8.34430	4.26696	7.13024	8.18817
S-S Ref. (Eltaher et al. 2023)	1	5.49920	8.86320	10.1046	5.47770	8.77250	9.96970
	4	4.52710	7.53980	8.67130	4.51510	7.48410	8.58640
	8	4.29300	7.24090	8.35930	4.27910	7.19170	8.28330
C-S	1	5.82138	8.89125	10.0885	5.76901	8.70174	9.80946
	4	4.90384	7.59199	8.67027	4.87264	7.47488	8.49478
	8	4.69100	7.30244	8.36238	4.66371	7.19837	8.20522
C-S Ref. (Eltaher et al. 2023)	1	6.30460	9.12880	10.2102	6.27220	9.02960	10.0709
	4	5.29740	7.80320	8.77670	5.27820	7.74140	8.68860
	8	5.06120	7.50960	8.46730	5.04440	7.45470	8.38830
C-C	1	6.34748	8.91423	10.1101	6.27944	8.72322	9.82926
	4	5.42364	7.62598	8.69586	5.38134	7.50726	8.51878
	8	5.21832	7.34205	8.39030	5.18068	7.23626	8.23153
C-C Ref. (Eltaher et al. 2023)	1	6.71140	9.32470	10.2941	6.67220	9.21890	10.1514
	4	5.70920	7.99610	8.86000	5.68510	7.92970	8.76940
	8	5.48330	7.70620	8.55250	5.46200	7.64670	8.47100

thereby reducing effective stiffness. Moreover, various figures are presented below to better interpret the effects of variables affecting the dimensionless frequency parameter.

Figure 3 displays the effect of changing the filling ratio of the perforated beam for the different number of holes on the dimensionless frequency parameter. For $N = 1$, the graph peaks at a certain α value and decreases, while as the number of holes grows, a clear increase curve emerges. Similar results have been also found by Assie et al. (2021). In this context, it is expected that frequencies will increase because the rise in the fill ratio enhances the structural continuity and effective stiffness of the beam. However, the observed increase–decrease behavior in the graphs indicates that the currently proposed formulations for perforated nanobeams yield more realistic and stable results, particularly after a certain number of holes. Accordingly, a hole count greater than 2 can be considered a critical threshold value at which these formulations can be reliably applied.

In Fig. 4, the change of dimensionless frequency parameters of the beams under different support conditions according to the change of α is presented. It has been observed that as fill ratio of perforated beam decreases, the dimensionless frequency parameters in different support conditions close each other. It is considered that this situation is related to the weakening of the beam's structural continuity due to a significant decrease in the fill ratio, and consequently, the near-complete elimination of the effect of boundary conditions on the free vibration behavior. Furthermore, as indicated in Fig. 3, the case where the number of

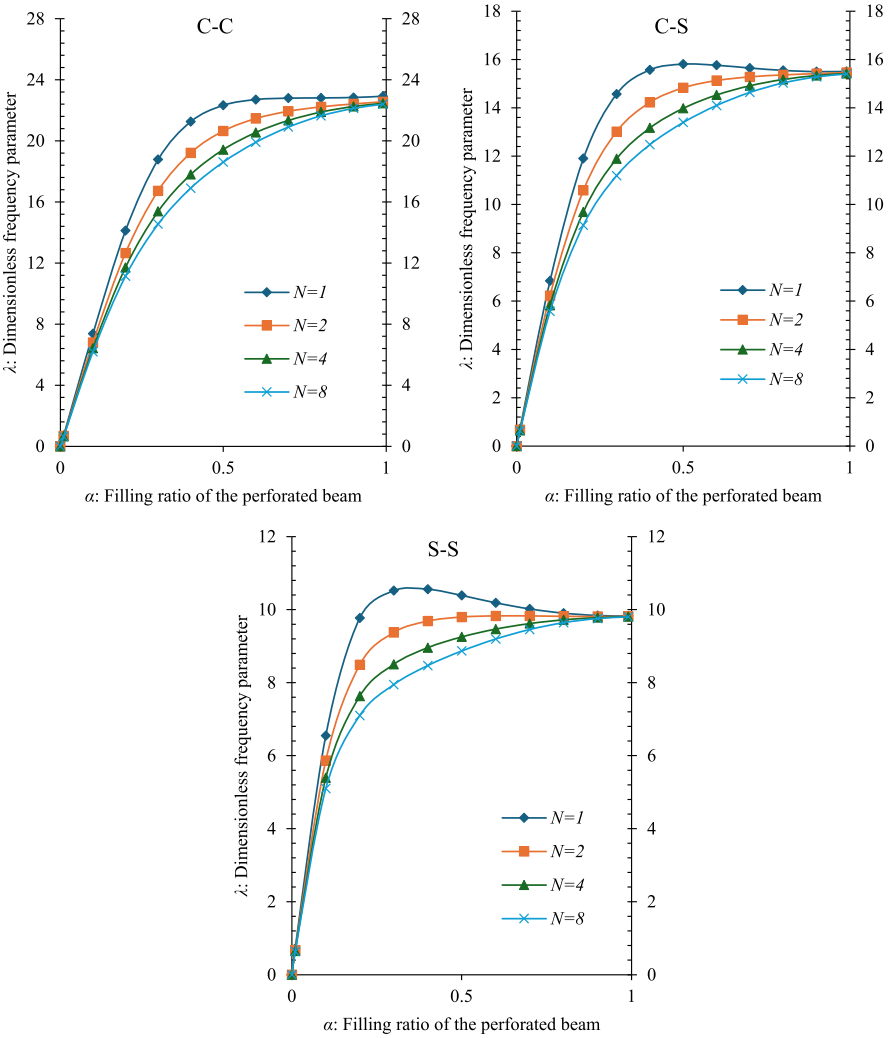


Fig. 3 Effect of the filling ratio variation on the dimensionless frequency parameter of the perforated beam (L = 10, L/h = 20, E = 30 MPa $\rho = 1$, $\nu = 0.3$, $\gamma = 0$)

holes exceeds 2 can be considered a significant indicator that the proposed formulations can represent the behavior of perforated beams more realistically. However, it can be stated that as the fill ratio exceeds 0.3, the effects of boundary conditions on system behavior become prominent once again.

Figure 5 indicates how the dimensionless frequency parameters change for different the filling ratio of perforated beam values depending on the number of holes. As the number of holes increased, the dimensionless frequency parameter decreased. This phenomenon is attributed to the fact that an increase in the number of holes increases structural discontinuity along the beam. Furthermore, a strong interaction between the fill ratio and the number of holes is clearly evident.

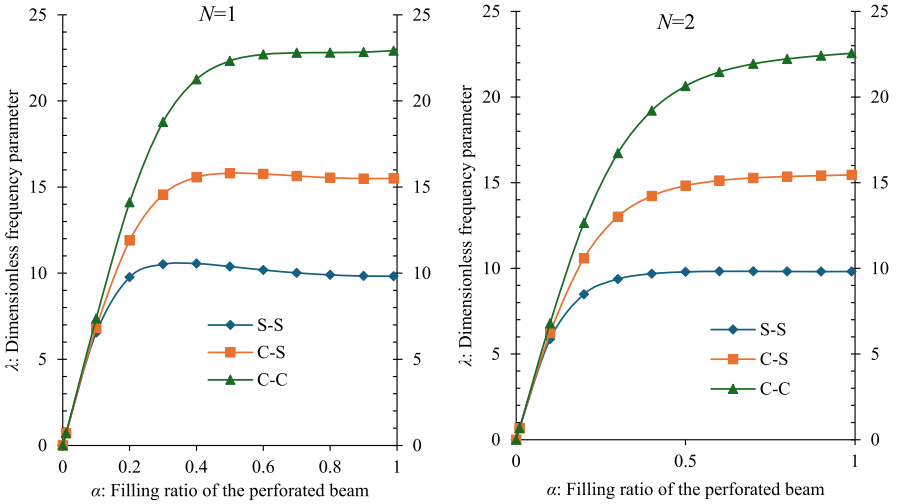


Fig. 4 Variation of the dimensionless frequency parameter of beams under different support conditions with respect to the filling ratio (L = 10, L/h = 20, E = 30 MPa $\rho = 1$, $\nu = 0.3$, $\gamma = 0$, $\tau = 0$)

Figure 6 displays how the dimensionless frequency parameter changes depending on the change of the number of holes for different support conditions. As number of holes increases, the dimensionless frequency parameter decreases asymptotically. In addition, since the effects of structural discontinuities become more pronounced under stiffer boundary conditions, the impact of an increase in the number of holes on system behavior is also more pronounced under stiffer boundary conditions. Additionally, as the filling ratio of perforated beam increases, the effect of the number of holes on the dimensionless frequency parameter also reduces.

Figure 7 presents a graph displaying the dimensionless frequency parameters of simply supported Timoshenko and Euler Bernoulli beams depending on L/h. Ks = 1000000 has been chosen to find the results according to Euler Bernoulli beam theory. It is seen that as the L/h ratio increases, the results obtained according to the two theories approach each other. When L/h $\geq$ 10, the results obtained according to these two theories are almost the same. This clearly demonstrates the inadequacy of Euler-Bernoulli beam theory for thick beams.

Figure 8 displays the effect of damping for different support conditions. According to this graph, it is seen that the effect of damping is greatest at more rigid boundary conditions. From a physical standpoint, it is known that beams with stiffer boundary conditions tend to dampen vibrational motion more quickly. The primary reason for this is that rigid support restricts structural motion more effectively and contributes to the faster dissipation of vibrational energy by reducing the system's deformation capacity. Especially in systems where viscoelastic behavior is considered, it is expected that energy dissipation mechanisms become more effective under rigid boundary conditions. Therefore, it can be stated that the results obtained are highly consistent with both mechanical behavior principles and physical reality. This observed trend also serves as an important validation, demonstrating that the proposed model and the solution approach used can successfully represent physical behavior.

Figure 9 indicates the effect of damping depending on the number of holes. It has been observed that the effect of damping decreases as the number of holes increases. This behav-

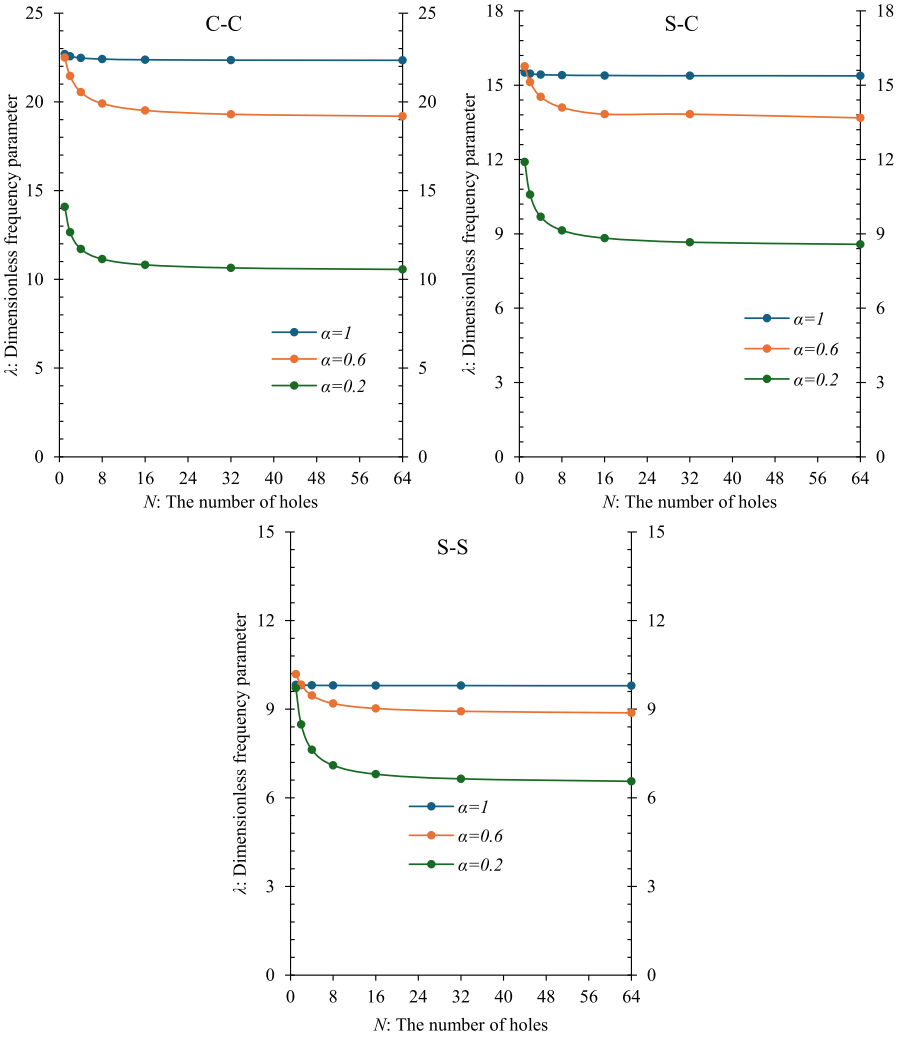


Fig. 5 Variation of the dimensionless frequency parameter with respect to the number of holes for different filling ratios (L = 10, L/h = 20, E = 30 MPa $\rho = 1$, $\nu = 0.3$, $\gamma = 0$, $\tau = 0$)

ior can be associated with the increase in structural discontinuities caused by the perforations distributed along the beam. As the number of holes increases, the effective stiffness and material continuity of the nanobeam are reduced, which alters the energy dissipation mechanism within the viscoelastic medium. Consequently, the contribution of the damping parameter to the overall dynamic response becomes less pronounced. In addition, for higher perforation densities, the structural response appears to be governed predominantly by geometric discontinuity effects rather than by viscoelastic damping characteristics. This trend indicates a significant interaction between perforation distribution and damping behavior in perforated viscoelastic nanobeams.

One of the main limitations of this study is that the material behavior is modeled within the framework of linear viscoelasticity combined with nonlocal elasticity theory. Although

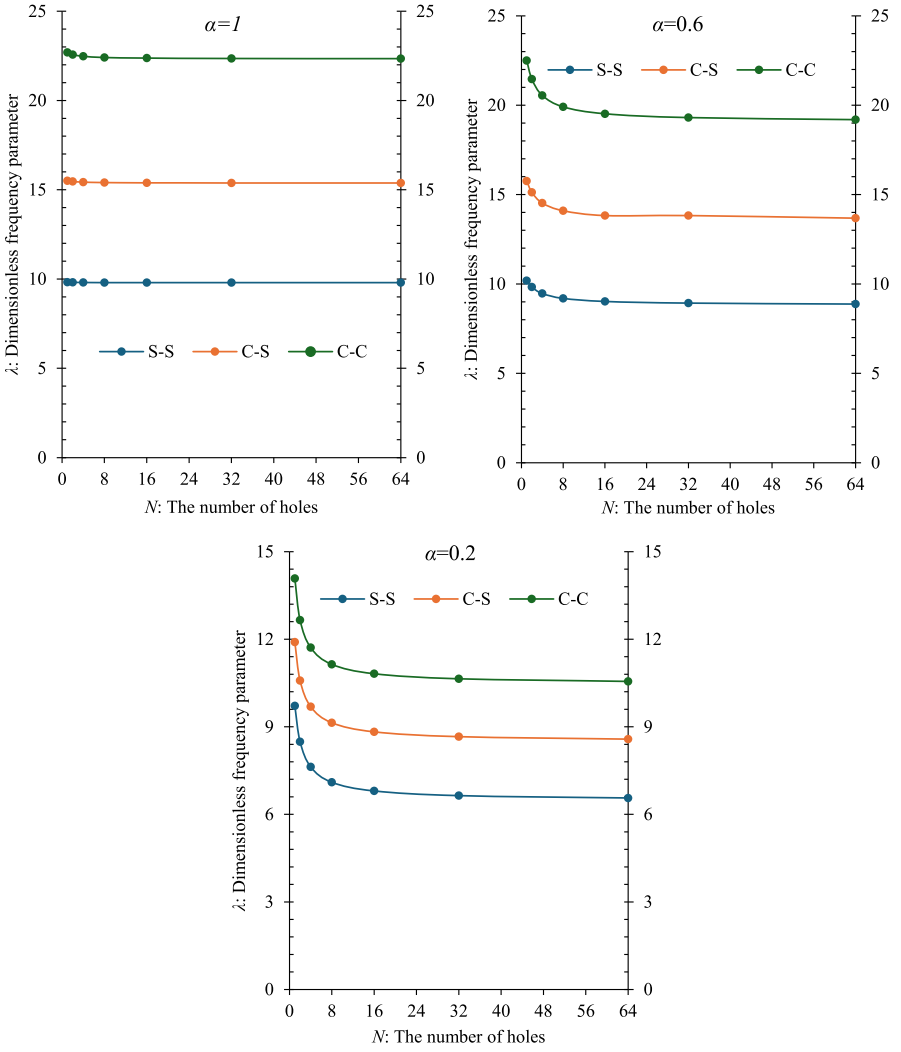


Fig. 6 Variation of the dimensionless frequency parameter with respect to the number of holes under different support conditions (L = 10, L/h = 20, E = 30 MPa $\rho = 1$, $\nu = 0.3$, $\gamma = 0$, $\tau = 0$)

this formulation is effective in capturing size-dependent effects at the nanoscale, other higher-order continuum approaches such as strain-gradient elasticity may also play an important role in describing nanoscale mechanical behavior, as they additionally incorporate strain gradient effects. In this context, the present study is restricted to the nonlocal elasticity framework, and strain-gradient effects are not considered. However, the proposed formulation can be extended in future work to include strain-gradient-based beam theories for a more comprehensive comparison of size-dependent models. In addition, nonlinear effects, temperature dependence, surface phenomena, and manufacturing imperfections are neglected, and perforations are represented through an equivalent homogenization approach. The study is also limited to free vibration analysis, while forced vibration and multi-physics interactions

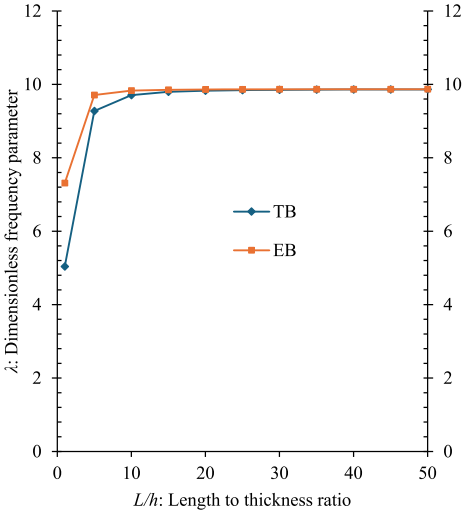


Fig. 7 The dimensionless frequency parameters of simply supported Timoshenko and Euler–Bernoulli beams with respect to the L/h ratio (h = b = 1, E = 30 MPa $\rho = 1$, $\nu = 0.3$, $\gamma = 0$, $\tau = 0$)

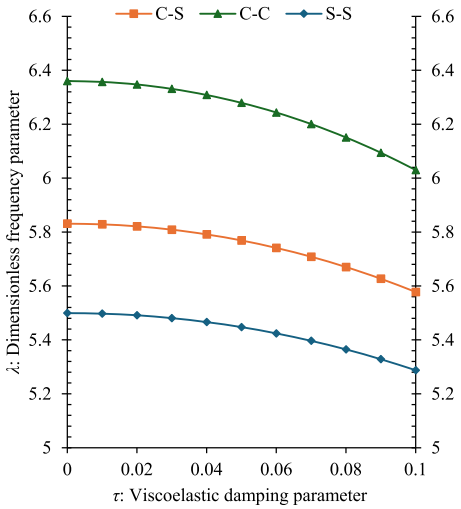


Fig. 8 The influence of viscoelastic damping parameter on the dynamic response under different support conditions (h = 1, b = h, L = 10 E = 30 MPa, $\nu = 0.3$, $\rho = 1$, $\alpha = 0.2$, $\gamma = 5$, N = 1)

are left for future investigations. Therefore, the results should be interpreted within these assumptions.

From a methodological perspective, the main contribution of this study is the development of a semi-analytical framework for perforated viscoelastic nonlocal Timoshenko nanobeams based on Fourier series expansion and the Stokes transform. This approach effectively reduces the governing high-order coupled differential equations to a single eigenvalue problem, ensuring both computational efficiency and accuracy. Furthermore, the method provides a unified formulation capable of handling different boundary conditions within the same mathematical structure. The simultaneous inclusion of nonlocal effects, viscoelastic behavior, and perforation-induced discontinuities within a single consistent model offers a comprehensive and efficient tool for the dynamic analysis of nanobeams.

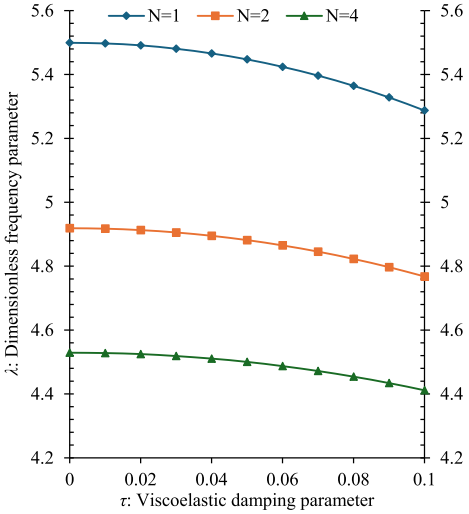


Fig. 9 Effect of the viscoelastic damping parameter on the dynamic response with respect to the number of holes for the S–S boundary condition (h = 1, b = h, L = 10 E = 30 MPa, $\nu = 0.3$, $\rho = 1$, $\alpha = 0.2$, $\gamma = 5$)

5 Conclusion

In this study, the free vibration behavior of perforated viscoelastic nonlocal Timoshenko nanobeams has been investigated using a semi analytic method based on the Fourier series and the Stokes transform. Thanks to the proposed solution approach, the equations of motion involving high-order differential equations were effectively reduced to a single eigenvalue problem, and results of high accuracy were obtained under various boundary conditions. Comparisons with existing studies in literature have demonstrated that the results obtained display a high degree of agreement, thereby validating the reliability of the developed method. In particular, it was observed that the Fourier series-based approach yields highly successful results under simply supported boundary conditions, while convergence is achieved with higher-order terms under clamped boundary conditions.

The results of parametric studies have revealed that an increase in the nonlocal scale parameter produces a significant softening effect on the system behavior, leading to a reduction in vibration characteristics. It was observed that this effect becomes particularly pronounced under stiffer boundary conditions. Furthermore, it was demonstrated that an increase in the viscoelastic damping parameter significantly suppresses the system's vibration behavior, and this effect is felt more strongly under rigid boundary conditions. However, it was determined that an increase in the number of holes reduces vibration characteristics due to the resulting increase in structural discontinuity. It was observed that as the perforation density increases, the viscoelastic damping effect weakens, and the system behavior is controlled more by geometric discontinuities.

The study has also determined that the effects of the boundary conditions, and shear deformation play a significant role in system behavior. It was observed that an increase in the fill ratio declines structural continuity, thereby strengthening system behavior, while at low fill ratios, the effect of boundary conditions weakens. Additionally, it was found that as the L/h ratio decreases, the effects of shear deformation become more pronounced, whereas at high L/h ratios, the Euler–Bernoulli and Timoshenko beam theories yield results that are quite close to one another.

When all the results are evaluated together, it is evident that the proposed method successfully captures the effects of nonlocal elasticity, viscoelastic behavior, and perforation

within a single formulation. In this regard, the study offers a reliable and computationally efficient alternative methodological approach with high convergence performance that can be used in the dynamic analysis of perforated nanostructures.

Author contributions All authors contributed equally to the study.

Funding information Open access funding provided by the Scientific and Technological Research Council of Türkiye (TÜBİTAK).

Data Availability No datasets were generated or analysed during the current study.

Declarations

Competing interests The authors declare no competing interests.

Open Access This article is licensed under a Creative Commons Attribution 4.0 International License, which permits use, sharing, adaptation, distribution and reproduction in any medium or format, as long as you give appropriate credit to the original author(s) and the source, provide a link to the Creative Commons licence, and indicate if changes were made. The images or other third party material in this article are included in the article's Creative Commons licence, unless indicated otherwise in a credit line to the material. If material is not included in the article's Creative Commons licence and your intended use is not permitted by statutory regulation or exceeds the permitted use, you will need to obtain permission directly from the copyright holder. To view a copy of this licence, visit http://creativecommons.org/licenses/by/4.0/.

References

Abdelrahman, A.A., Esen, I., Daikh, A.A., Eltaher, M.A.: Dynamic analysis of FG nanobeam reinforced by carbon nanotubes and resting on elastic foundation under moving load. Mech. Based Des. Struct. Mach. **51**, 5383–5406 (2023). https://doi.org/10.1080/15397734.2021.1999263

Abdullah, S.S., Hashemi, S.H., Hussein, N.A., Nazemnezhad, R.: Effect of thermal axial load on vibration of cracked single-walled carbon nanotubes modelled as Timoshenko nanobeams using nonlocal theory. Aust. J. Mech. Eng. **21**, 860–871 (2023). https://doi.org/10.1080/14484846.2021.1918363

Amir, S., Soleimani-Javid, Z., Arshid, E.: Size-dependent free vibration of sandwich micro beam with porous core subjected to thermal load based on SSDBT. Z. Angew. Math. Mech. **99**, e201800334 (2019). https://doi.org/10.1002/zamm.201800334

Ansari, R., Faraji Oskouie, M., Sadeghi, F., Bazdid-Vahdati, M.: Free vibration of fractional viscoelastic Timoshenko nanobeams using the nonlocal elasticity theory. Physica E, Low-Dimens. Syst. Nanostruct. **74**, 318–327 (2015). https://doi.org/10.1016/j.physe.2015.07.013

Artan, R., Tepe, A.: In-plane static behavior of nonlocal curved nanobeams resting on an elastic foundation determined using the initial value method. J. Elast. **157**, 49 (2025). https://doi.org/10.1007/s10659-025-10140-w

Assie, A., Akbaş, Ş.D., Bashiri, A.H., Abdelrahman, A.A., Eltaher, M.A.: Vibration response of perforated thick beam under moving load. Eur. Phys. J. Plus **136**, 283 (2021). https://doi.org/10.1140/epjp/s13360-021-01224-2

Attia, M.A., Abdel Rahman, A.A.: On vibrations of functionally graded viscoelastic nanobeams with surface effects. Int. J. Eng. Sci. **127**, 1–32 (2018). https://doi.org/10.1016/j.ijengsci.2018.02.005

Azimi, M., Mirjavadi, S.S., Shafiei, N., Hamouda, A.M.S., Davari, E.: Vibration of rotating functionally graded Timoshenko nano-beams with nonlinear thermal distribution. Mech. Adv. Mater. Struct. **25**, 467–480 (2018). https://doi.org/10.1080/15376494.2017.1285455

Challamel, N., Kaci, A., Tounsi, A.: Exact solutions for the static bending of nonlocal higher-order shear beams under various boundary conditions. Mech. Adv. Mater. Struct. **32**, 6132–6148 (2025). https://doi.org/10.1080/15376494.2025.2521837

Civalek, Ö., Şeker, M., Numanoğlu, H.M.: In-plane free vibration analysis of nonlocal nanorings embedded in elastic medium. Appl. Phys. A **131**, 69 (2025). https://doi.org/10.1007/s00339-024-08204-0

Czekanski, A., Zozulya, V.V.: Vibration analysis of nonlocal beams using higher-order theory and comparison with classical models. Mech. Adv. Mater. Struct. **28**, 1293–1309 (2021). https://doi.org/10.1080/15376494.2019.1665761

Dalgıç, A.M., Tüfekci, M., Pir, İ., Tüfekci, E.: Exact analytical solutions for static response of helical single-walled carbon nanotubes using nonlocal Euler–Bernoulli beam theory. Nanomaterials **15**, 1461 (2025). https://doi.org/10.3390/nano15191461

Eltaher, M.A., Alshorbagy, A.E., Mahmoud, F.F.: Vibration analysis of Euler–Bernoulli nanobeams by using finite element method. Appl. Math. Model. **37**, 4787–4797 (2013). https://doi.org/10.1016/j.apm.2012.10.016

Eltaher, M.A., Omar, F.-A., Abdalla, W.S., Gad, E.H.: Bending and vibrational behaviors of piezoelectric nonlocal nanobeam including surface elasticity. Waves Random Complex Media **29**, 264–280 (2019). https://doi.org/10.1080/17455030.2018.1429693

Eltaher, M.A., Shanab, R.A., Mohamed, N.A.: Analytical solution of free vibration of viscoelastic perforated nanobeam. Arch. Appl. Mech. **93**, 221–243 (2023). https://doi.org/10.1007/s00419-022-02184-4

Eringen, A.C.: Nonlocal polar elastic continua. Int. J. Eng. Sci. **10**, 1–16 (1972). https://doi.org/10.1016/0020-7225(72)90070-5

Eringen, A.C., Edelen, D.G.B.: On nonlocal elasticity. Int. J. Eng. Sci. **10**, 233–248 (1972). https://doi.org/10.1016/0020-7225(72)90039-0

Ghadiri, M., Hosseini, S.H.S., Shafiei, N.: A power series for vibration of a rotating nanobeam with considering thermal effect. Mech. Adv. Mater. Struct. **23**, 1414–1420 (2016). https://doi.org/10.1080/15376494.2015.1091527

Hosseini, S.a.H., Rahmani, O., Bayat, S.: A new solution for dynamic response of FG nonlocal beam under moving harmonic load. Steel Compos. Struct. **43**, 185–200 (2022)

Hosseini-Hashemi, S., Behdad, S., Fakher, M.: Vibration analysis of two-phase local/nonlocal viscoelastic nanobeams with surface effects. Eur. Phys. J. Plus **135**, 190 (2020). https://doi.org/10.1140/epjp/s13360-020-00148-7

Kadioglu, H.G.: A Fourier series-based approach for the size-dependent free vibration of viscoelastic microbeams. Int. J. Mech. Mater. Des. **22**, 91 (2026). https://doi.org/10.1007/s10999-026-09908-2

Kadıoğlu, H., Yaylı, M.Ö.: Buckling analysis of non-local Timoshenko beams by using Fourier series. Int. J. Eng. Appl. Sci. **9**, 89–99 (2017). https://doi.org/10.24107/ijeas.362242

Kadioglu, H.G., Yayli, M.O.: Axial vibration of a viscoelastic FG nanobeam with arbitrary boundary conditions. J. Vib. Eng. Technol. **13**, 96 (2025). https://doi.org/10.1007/s42417-024-01671-y

Karličić, D., Cajić, M., Murmu, T., Adhikari, S.: Nonlocal longitudinal vibration of viscoelastic coupled double-nanorod systems. Eur. J. Mech. A Solids **49**, 183–196 (2015). https://doi.org/10.1016/j.euromechsol.2014.07.005

Ke, L.L., Xiang, Y., Yang, J., Kitipornchai, S.: Nonlinear free vibration of embedded double-walled carbon nanotubes based on nonlocal Timoshenko beam theory. Comput. Mater. Sci. **47**, 409–417 (2009). https://doi.org/10.1016/j.commatsci.2009.09.002

Khaniki, H.B.: On vibrations of nanobeam systems. Int. J. Eng. Sci. **124**, 85–103 (2018). https://doi.org/10.1016/j.ijengsci.2017.12.010

Lee, H.-L., Chang, W.-J.: Surface effects on frequency analysis of nanotubes using nonlocal Timoshenko beam theory. J. Appl. Phys. **108**, 093503 (2010). https://doi.org/10.1063/1.3503853

Lei, Y., Murmu, T., Adhikari, S., Friswell, M.I.: Dynamic characteristics of damped viscoelastic nonlocal Euler–Bernoulli beams. Eur. J. Mech. A Solids **42**, 125–136 (2013a). https://doi.org/10.1016/j.euromechsol.2013.04.006

Lei, Y., Adhikari, S., Friswell, M.I.: Vibration of nonlocal Kelvin-Voigt viscoelastic damped Timoshenko beams. Int. J. Eng. Sci. **66–67**, 1–13 (2013b). https://doi.org/10.1016/j.ijengsci.2013.02.004

Martin, O.: Nonlinear vibrations of fractional nonlocal viscoelastic nanotube resting on a Kelvin-Voigt foundation. Mech. Adv. Mater. Struct. **29**, 2769–2779 (2022). https://doi.org/10.1080/15376494.2021.1878401

Mohamed, S.A., Shanab, R.A., Seddek, L.F.: Vibration analysis of Euler–Bernoulli nanobeams embedded in an elastic medium by a sixth-order compact finite difference method. Appl. Math. Model. **40**, 2396–2406 (2016). https://doi.org/10.1016/j.apm.2015.08.019

Mohammadimehr, M., Monajemi, A.A., Afshari, H.: Free and forced vibration analysis of viscoelastic damped FG-CNT reinforced micro composite beams. Microsyst. Technol. **26**, 3085–3099 (2020). https://doi.org/10.1007/s00542-017-3682-4

Murmu, T., Adhikari, S.: Nonlocal transverse vibration of double-nanobeam-systems. J. Appl. Phys. **108**, 083514 (2010). https://doi.org/10.1063/1.3496627

Nejad, M.Z., Hadi, A.: Non-local analysis of free vibration of bi-directional functionally graded Euler–Bernoulli nano-beams. Int. J. Eng. Sci. **105**, 1–11 (2016). https://doi.org/10.1016/j.ijengsci.2016.04.011

r. Ebrahimian, M., Imam, A., Najafi, M.: Doublet mechanical analysis of bending of Euler-Bernoulli and Timoshenko nanobeams. Z. Angew. Math. Mech. **98**, 1642–1665 (2018). https://doi.org/10.1002/zamm.201700365

Reddy, J.N.: Nonlocal theories for bending, buckling and vibration of beams. Int. J. Eng. Sci. **45**, 288–307 (2007). https://doi.org/10.1016/j.ijengsci.2007.04.004

Reddy, J.N.: Microstructure-dependent couple stress theories of functionally graded beams. J. Mech. Phys. Solids **59**, 2382–2399 (2011). https://doi.org/10.1016/j.jmps.2011.06.008

Roudbari, M.A., Jorshari, T.D., Lü, C., Ansari, R., Kouzani, A.Z., Amabili, M.: A review of size-dependent continuum mechanics models for micro- and nano-structures. Thin-Walled Struct. **170**, 108562 (2022). https://doi.org/10.1016/j.tws.2021.108562

Shanab, R.A., Mohamed, S.A., Mohamed, N.A., Attia, M.A.: Comprehensive investigation of vibration of sigmoid and power law FG nanobeams based on surface elasticity and modified couple stress theories. Acta Mech. **231**, 1977–2010 (2020). https://doi.org/10.1007/s00707-020-02623-9

Shen, Z.-B., Li, X.-F., Sheng, L.-P., Tang, G.-J.: Transverse vibration of nanotube-based micro-mass sensor via nonlocal Timoshenko beam theory. Comput. Mater. Sci. **53**, 340–346 (2012). https://doi.org/10.1016/j.commatsci.2011.09.023

Sheykhi, M., Eskandari, A., Ghafari, D., Ahmadi Arpanahi, R., Mohammadi, B., Hosseini Hashemi, Sh.: Investigation of fluid viscosity and density on vibration of nano beam submerged in fluid considering nonlocal elasticity theory. Alex. Eng. J. **65**, 607–614 (2023). https://doi.org/10.1016/j.aej.2022.10.016

Son, L.T., Belarbi, M.-O., Tounsi, A., Ziou, H., Avcar, M., Van Vinh, P.: Nonlocal vibration analysis of functionally graded sandwich nanoplates resting on general viscoelastic foundations. Mech. Adv. Mater. Struct. 1–18 (2025). https://doi.org/10.1080/15376494.2025.2521729

Tariq, A., Kadıoğlu, H.G., Uzun, B., Deliktaş, B., Yaylı, M.Ö.: Modeling the viscoelastic behavior of a FG nonlocal beam with deformable boundaries based on hybrid machine learning and semi-analytical approaches. Arch. Appl. Mech. **95**, 79 (2025). https://doi.org/10.1007/s00419-025-02776-w

Tepe, A.: Nonlocal effects on curved double-walled carbon nanotubes based on nonlocal theory. Arch. Appl. Mech. **95**, 57 (2025). https://doi.org/10.1007/s00419-025-02762-2

Trabelssi, M., El-Borgi, S., Fernandes, R., Ke, L.-L.: Nonlocal free and forced vibration of a graded Timoshenko nanobeam resting on a nonlinear elastic foundation. Composites, Part B, Eng. **157**, 331–349 (2019). https://doi.org/10.1016/j.compositesb.2018.08.132

Uymaz, B.: Forced vibration analysis of functionally graded beams using nonlocal elasticity. Compos. Struct. **105**, 227–239 (2013). https://doi.org/10.1016/j.compstruct.2013.05.006

Uzun, B., Yaylı, M.Ö.: Nonlocal vibration analysis of Ti-6Al-4V/ZrO2 functionally graded nanobeam on elastic matrix. Arab. J. Geosci. **13**, 155 (2020). https://doi.org/10.1007/s12517-020-5168-4

Uzun, B., Yaylı, M.Ö., Deliktaş, B.: Free vibration of FG nanobeam using a finite-element method. Micro Nano Lett. **15**, 35–40 (2020). https://doi.org/10.1049/mnl.2019.0273

Uzun, B., Civalek, Ö., Yaylı, M.Ö.: Vibration of FG nano-sized beams embedded in Winkler elastic foundation and with various boundary conditions. Mech. Based Des. Struct. Mach. **51**, 481–500 (2023). https://doi.org/10.1080/15397734.2020.1846560

Wang, C.M., Zhang, Y.Y., He, X.Q.: Vibration of nonlocal Timoshenko beams. Nanotechnology **18**, 105401 (2007). https://doi.org/10.1088/0957-4484/18/10/105401

Yayli, M.Ö.: On the axial vibration of carbon nanotubes with different boundary conditions. Micro & Nano Letters **9**, 807–811 (2014). https://doi.org/10.1049/mnl.2014.0398

Yayli, M.Ö.: Buckling analysis of a microbeam embedded in an elastic medium with deformable boundary conditions. Micro Nano Lett. **11**, 741–745 (2016). https://doi.org/10.1049/mnl.2016.0257

Yayli, M.Ö.: Torsional vibration analysis of nanorods with elastic torsional restraints using non-local elasticity theory. Micro Nano Lett. **13**, 595–599 (2018). https://doi.org/10.1049/mnl.2017.0751

Zhang, G., Gao, X.-L.: A new Bernoulli–Euler beam model based on a reformulated strain gradient elasticity theory. Math. Mech. Solids **25**, 630–643 (2020). https://doi.org/10.1177/1081286519886003

Zhang, J.-Q., Qing, H., Gao, C.-F.: Exact and asymptotic bending analysis of microbeams under different boundary conditions using stress-derived nonlocal integral model. Z. Angew. Math. Mech. **100**, e201900148 (2020). https://doi.org/10.1002/zamm.201900148

Publisher's note Springer Nature remains neutral with regard to jurisdictional claims in published maps and institutional affiliations.